IEEE Access
Multidisciplinary ⋮ Rapid Review ⋮ Open Access Journal

Received 28 June 2024, accepted 15 July 2024, date of publication 18 July 2024, date of current version 2 September 2024.

Digital Object Identifier 10.1109/ACCESS.2024.3430934

RESEARCH ARTICLE

Recognition of Emotional Categories Using Mined Fuzzy Rules From Electroencephalogram Signals With Gated Eye Track Data Approach

JAVID FARHADI SEDEHI, NADER JAFARNIA DABANLOO, KEIVAN MAGHOOLI, AND ALI SHEIKHANI
Department of Biomedical Engineering, Science and Research Branch, Islamic Azad University, Tehran 14778-93855, Iran
Corresponding author: Nader Jafarnia Dabanloo (jafarnia@srbiau.ac.ir)

This work was supported by the Science and Research Branch, Islamic Azad University.

This work involved human subjects or animals in its research. The authors confirm that all human/animal subject research procedures and protocols are exempt from review board approval.

ABSTRACT Researchers suggest that a short video clip, when tagged with a single label, is sufficient for classification into an emotional category. However, when subjects view an emotional film tagged similarly, there is no guarantee that the designated emotion persists throughout the duration, or when exactly the emotion is elicited. This inconsistency adversely affects the performance of emotion recognition (ER) systems. In this study, we propose a multimodal ER system employing an eye-tracking gated strategy to identify the most effective timing for emotional categorization. Initially, common eye-tracking features are extracted and selected using the minimum-redundancy-maximum-relevance (mRMR) method. Subsequently, the most discriminative feature is employed as a threshold to pinpoint the most relevant timing. EEG signals from these moments are then decomposed into five standard frequency bands using the Daubechies wavelet function (order 4). Furthermore, four types of entropy features are extracted from four-second segments of 62 and 32 channels for the SEED-IV and MAHNOB-HCI databases, respectively. The best features, as determined by the mRMR method, are fed into a Sugeno-fuzzy inference system (S-FIS) designed to derive rules for discriminating between the four emotional categories of happiness, fear, sadness, and neutrality. The S-FIS rules were refined using a genetic algorithm (GA), leading to most discriminative rules achieving average accuracies of 94.42% and 85.20% for the alpha frequency bands of the SEED-IV and MAHNOB-HCI databases, respectively. The results of this study demonstrate the effectiveness of fuzzy rule extraction in enhancing the performance of multimodal ER systems

INDEX TERMS Electroencephalogram (EEG), emotion recognition, Sugeno-fuzzy inference system (S-FIS), entropy, mine fuzzy rule.

I. INTRODUCTION

This study introduces a novel method to explore various dimensions, beginning with the expression and delineation of uncertainty in emotion classification to address issues associated with probability theory. Recognizing that expert involvement or access to a knowledge base enhances problem-solving, establishing a comprehensive rule base marks a significant shift in emotion recognition (ER). This allows for the effective use of knowledge and benefits emotion research and disease diagnosis [1], [2], [3]. Furthermore, given the interdependence of brain and biological signals, analyzing a single signal is insufficient. A holistic approach considers the interactions between different physiologic signals. This involves examining how an emotional stimulus may alter the strength of one signal in relation to another,

The associate editor coordinating the review of this manuscript and approving it for publication was Yu-Da Lin.

showcasing the complex interplay of physiological responses. In this study we have used multimodal databases including electroencephalogram (EEG) and eye track data. There are multiple brain imaging techniques to investigate emotional states, including EEG [1], [2], [3], functional magnetic resonance imaging (fMRI) [4], magnetoencephalography (MEG) [5], and near-infrared spectroscopy (NIRS) [6]. Among these, EEG stands out due to its higher temporal resolution. Additionally, EEG is widely available in most research and academic centers and is more cost-effective. Moreover, eye track is a novel and interesting modality that has been augmented information in neuroscience studies. Recently, this modality has been used to improve performance of ER [7], [8], [9] and evaluate autism [10], [11]. One of the study's highlights is identifying timing of eliciting emotions from eye track data. Finding interactions between EEG signal and eye track signal, crucial for refining classification accuracy and identifying brain regions activated by stimuli, such as watching a thriller. Additionally, measuring changes in pupil diameter or blink rate and linking these to specific events aids in pinpointing brain areas that significantly influence accuracy. In summary, this research not only tackles theoretical challenges but also introduces practical methods for unraveling the intricate links between emotional and physiological responses, advancing our understanding and potential diagnostic applications.

ER from multimodal signals is a cutting-edge field that merges neuroscience, psychology, and technology to understand human emotions through brainwave patterns. This interdisciplinary approach has a wide range of applications across various sectors. Here are some key applications:

- EEG-based emotion recognition can aid in diagnosing mental health conditions such as depression [12], [13] and anxiety [14], [15] by identifying abnormal emotional responses. It can also monitor the effectiveness of treatments by observing changes in emotional states over time.
- In human-computer interaction (HCI), EEG-based emotion recognition can enable systems to adapt in real-time to the user's emotional state, improving user experience. For example, a learning application could adjust its difficulty level or content presentation style based on the learner's frustration or engagement levels [16], [17].
- Video game developers can use ER system to create more immersive and responsive gaming experiences that adapt to the player's emotional state, enhancing engagement and satisfaction [18].

The contribution of this study is as follows:

-Developing a multimodal and multiclass Emotion Recognition (ER) system using eye-tracking data as a gated strategy and EEG signals as input. This study investigates the best eye-tracking features through a powerful machine learning technique to extract relevant emotional aspects from EEG signals.

-Enhancing the performance of discriminating between multiclass emotional categories from two multimodal databases by integrating machine learning techniques with fuzzy logic. Machine learning techniques included extract nonlinear features of entropy and select best features using the minimum Redundancy Maximum Relevance (mRMR) method. Then, the best features used as inputs for fuzzy logic, which then mines effective fuzzy rules for multiclass emotional categories.

-Addressing the uncertainties of emotional categories using a type 1 Sugeno-fuzzy inference system (S-FIS). Unlike traditional studies that rely on neural networks' black-box models, this approach leverages fuzzy logic to mine high-level expert knowledge about data patterns. Furthermore, the S-FIS is optimized with a genetic algorithm to discover the most effective fuzzy rules for distinguishing between multiple emotion classes.

-Evaluating the proposed method on two public databases, MAHNOB-HCI and SEED-IV, focusing on four emotional categories from the first database and sadness, happiness, fear and neutrality.

II. RELATED STUDIES

Zheng et al. [19] introduced an ER technique combining EEG signals and eye tracker-derived pupillary response data. They used 15 emotional film clips to elicit positive, neutral, and negative states from 5 subjects, extracting features such as power spectral density (PSD), differential entropy (DE), and asymmetry measures. Employing linear dynamic system (LDS) for EEG smoothing and a support vector machine (SVM) for classification, they achieved highest accuracies of 71.77% (EEG) and 58.90% (eye-tracking), with a feature-level fusion strategy further increasing accuracy to 73.59%. Su et al. [20] proposed a method to perceive multi-modal emotion intensity by integrating EEG and eye movement data. They developed a stimulus selection method for evoking various emotional states in a study involving twelve participants and forty emotional trials. They extracted feature parameters such as average power spectral (APS) and average energy (AE) from different brain frequency bands. Using a two-classification SVM approach, they assessed emotion intensity across arousal and valence dimensions. Separate classifiers for EEG and eye movement data were used before combining them through decision-level fusion, aiming to enhance recognition accuracy. The highest recognition accuracies achieved for arousal and valence dimensions were 72.8% and 69.3%, respectively, in a laboratory setting. Li et al. [21] studied the use of EEG and eye movement signals for classifying five emotions (happy, sad, fear, disgust, neutral) over time, creating the SEED-V dataset from 16 subjects. They extracted DE from EEG across five frequency bands and computed 33-dimensional eye movement features (including pupil diameter and saccade) through statistical analysis. SVM and MLP classifiers were trained on EEG and eye movement signals, respectively. They also combined EEG and eye movement features using a feature-level fusion (FLF) method. The study found average accuracies of 70.8%

(EEG), 59.87% (eye movement), and 75.13% (FLF). Gong et al. [22] investigated emotion cognition across cultural groups using EEG and eye movement signals on SEED-CHN, SEED-GER, and SEED-FRA datasets, focusing on intracultural and cross-cultural analyses. They extracted DE from EEG and various features from eye movements, employing a neural network called multiple stacked broad learning system (MSBLS) for fusion, achieving high accuracies in cultural settings: 94.30% (Chinese), 94.33% (German), and 84.68% (French). Zhu et al. [23] integrated EEG and eye-tracking for product evaluation, predicting valence and arousal from EEG and deriving preferences through statistical analysis and a spatial-temporal neural network, Att-2DCNN, achieving maximum accuracies of 93.71% and 93.56% for valence and arousal, and 95.12% for design decision prediction through fusion of EEG and eye-tracking. Fu et al. [24] proposed a Multimodal Feature Fusion Neural Network (MFFNN) for ER from EEG and eye movement, achieving an 87.32% accuracy on the SEED-IV dataset for four emotions through dual-branch feature extraction and multi-scale feature fusion. Lu et al. [25] aimed to improve ER by combining eye movements and EEG, exploring features and fusion strategies for three emotions: positive, negative, and neutral. They extracted 16 eye movement features and EEG features like PSD and DE, using an SVM with a linear kernel for classification. Various fusion strategies, including FLF and DLF, were tested. The fuzzy integral fusion strategy yielded the highest accuracy at 87.59%, compared to 77.80% with eye movements alone and 78.51% with EEG data alone. Antoniou et al. [26] developed a brain-computer interface (BCI) system using the Emotiv EPOC Flex to capture EEG signals and classify them into six categories related to eye movements (open, closed, left, right, up, and down) using the random forests (RF) algorithm. After preprocessing and feature extraction, the method achieved an accuracy of 85.39%, surpassing other classification algorithms. Zheng et al. [7] developed a multimodal framework to recognize four emotions (happy, sad, fear, and neutral) that integrated EEG signals and eye movements. They used PSD and DE for EEG signals, and various detailed parameters for eye movements, such as pupil diameters, fixation details, saccade details, blink details, and event statistics. The classification methods involved modality fusion using multimodal deep learning and feature-level fusion approaches. The results showed that modality fusion significantly improved classification accuracies, with an average accuracy of 85.11% for recognizing the four emotions. Zhou et al. [27] introduced a multimodal fusion framework for Emotion Recognition (ER) using EEG and eye movement signals, focusing on four emotions (happy, sad, fear, neutral) with the SEED-IV dataset. Their SOFNN (subjective and objective signal fusion) framework effectively extracted temporal-spatial features, showing improved classification for neutral and fear emotions, with moderate success for sad emotions. The highest accuracy achieved was 86.27%.

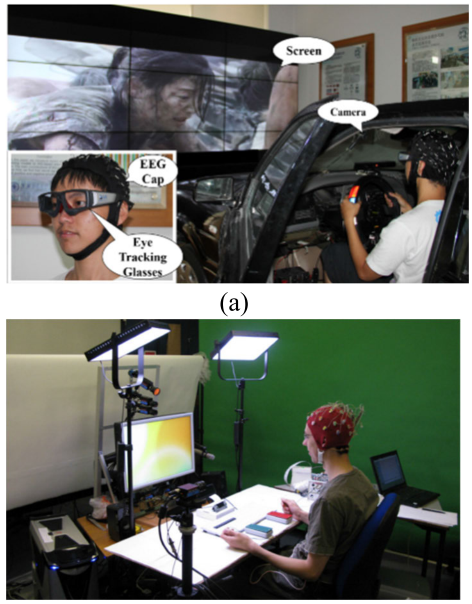

(a)

(b)

FIGURE 1. An example of recording devices and environment from (a) the SEED-IV [7] and (b) MAHNOB-HCI databases [9].

III. MATERIAL AND METHODS

A. MULTIMODAL SEED-IV DATABASE

This database is recorded from 15 (8 female/ 7 male) healthy subjects with average age of 21.32 old, while watching 72 short emotional clips [7]. EEG signals from 62 locations according to 10-20 electrode placement system were recorded with 1000 sampling frequency. EEG signals were recorded using the ESI NuroScan device with Ag/Ag-CL electrodes. Four discrete emotional categories, sadness, happiness, fear and neutral were considered among clips. Duration of clips were between 48 seconds to 3 minutes (short clips were selected to elicit only one category of emotions). Also, eye-track data has been recorded simultaneously by the SMI eye-tracking glass. FIGURE 1 shows the environment of recording EEG and eye-track data for the SEED-IV (a) and MAHNOB-HCI (b). Table 1 report details of this database.

B. MULTIMODAL MAHNOB-HCI DATABASE

The MAHNOB-HCI database comprises EEG recordings from 27 healthy participants, captured across 32 channels while they viewed 20 different video clips [9]. The participant group consisted of 16 females and 11 males with varied educational backgrounds, aged between 19 and 40 years (mean age = 26.06, standard deviation = 4.39). The EEG data were collected using a Biosemi Active II system, adhering to the 10–20 international electrode placement standard, at a sampling frequency of 256 Hz. The selection of video clips, derived from a preliminary study and including online and weather forecast segments, is detailed in [9]. The protocol to elicit various emotional responses involved three steps: 1) presenting a neutral clip to mitigate emotional

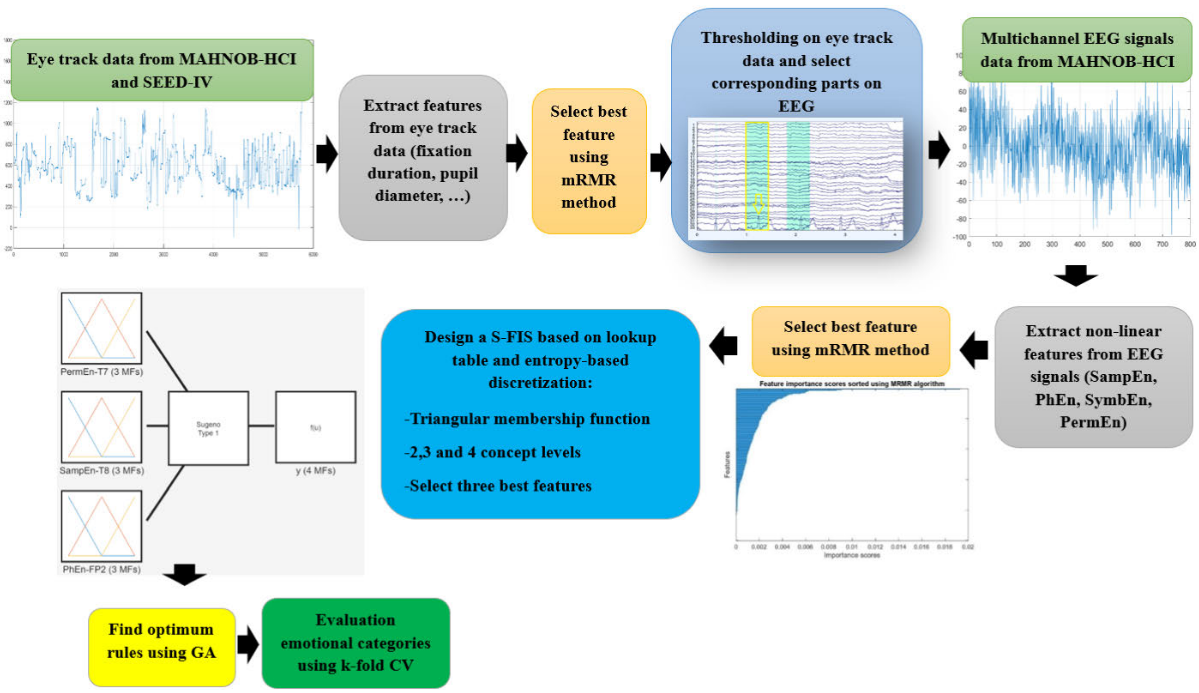

FIGURE 2. Proposed eye track data gated EEG-S-FIS-GA-ER system from MAHNOB-HCI and SEED-IV databases.

TABLE 1. Details of SEED-IV and MAHNOB-HCI multimodal databases.

Database	Subjects (f/m)	Age (m± std)	Nationality	Length of signal (second)	# samples	Sampling frequency
SEED-IV	8/ 7	21.32 ± 2.45	Chinese	48-300	62 EEG channels, eye track signal	1000 (200Hz)
MAHNOB-HCI	16/11	26.06± 4.39	European	34-117	32 EEG channels, 43 eye gaze data	256 Hz

preconceptions, 2) displaying emotional video clips, and 3) completing a self-assessment form. Each participant's session lasted approximately 50 minutes, with individual trials around two and a half minutes. The durations of the video clips ranged from approximately 34 to 117 seconds.

C. EMOTION CATEGORIES

According to Ekman's theory, sadness, happiness, and fear are fundamental emotional categories universally recognized across different nationalities [28]. In other words, these emotions exhibit similarities among individuals regardless of sex, culture, or age. This study focuses on classifying these emotions, along with neutrality, as they represent core affective states that are commonly understood and identifiable across diverse demographic groups. By examining these basic emotions, the study aims to contribute to a deeper understanding of emotional processing and recognition, which could have broad implications for fields such as psychology, neuroscience, and human-computer interaction.

D. PROPOSED S-FIS-GA-ER SCHEMA

In this study, we proposed a multimodal ER system that provides selected parts of EEG signals based on eye track data. In the other words, this system determined a threshold based on a specific feature extracted from eye track data, then, select corresponding parts from EEG signals which are most effective parts in recognition of four desired emotional categories i.e., sadness, happiness, fear and neutrality. Then, nonlinear features are extracted from these EEG signals and after selection of three best features using desired feature selection method, a S-FIS is designed to mine rules. This S-FIS is tunes using the GA and optimized rules are used to discriminate four mentioned emotional categories. FIGURE 2 illustrates these steps.

E. EYE TRACKER AS A GATEWAY FOR SELECTING PHYSIOLOGICAL SIGNALS

In this step, eye track data is used to select most discriminative parts of EEG signals to be processes in our multiclass ER problem. To do this work, appropriate features according to [7] are extracted from eye track data.

1) EXTRACT FEATURES

These features include average and standard deviation of fixation duration and pupil diameter (in X and Y directions), fixation frequency and maximum fixation duration [7].

Fixation duration refers to the amount of time (milli second) that the eyes remain stationary, focusing on a single point or area in the visual field. Longer fixation durations can indicate more in-depth cognitive processing, difficulty in understanding, or heightened interest in the visual content. Average of fixation duration computes sum of duration of all fixation divided by number of fixations in the trial according to milli second. Fixation frequency refers to the number of fixations that occur within a given time frame or during a particular task. Maximum fixation duration is the length of the longest single fixation recorded during a specific period or task. This feature indicates the point of greatest interest, difficulty, or engagement within the visual field. pupil diameter refers to the measurement of the width of the pupil, in each X and Y directions. Pupil diameter can vary based on several factors, including light levels (pupillary light reflex), emotional state, cognitive load, and other physiological and psychological conditions. Finally, 8 features are extracted from every 4 second segments, length of segments are selected to compare with [7].

2) SELECT FEATURES USING mRMR METHOD

After extract mentioned features, the mRMR [29] is used to select best features in each database. The mRMR feature selection approach systematically identifies a set of features characterized by minimal mutual redundancy while maximizing the mutual information with the outcome variable (class label) [29]. Mutual information between two features, denoted as x and y, is quantitatively defined in Eq (1). This equation employs the probability density functions (PDFs) $p(x)$, $p(y)$ and $p(x, y)$ to measure the statistical dependence or information shared between the features. The core principle of mRMR is to enhance the predictive power of models by selecting features that offer the most unique and relevant information about the target variable [29].

$$I(x; y) = \iint p(x, y) \log \frac{p(x, y)}{p(x)\, p(y)} d_x d_y \tag{1}$$

The quantification of the maximal correlation or dependency between the feature set and the class label is achieved through the application of Eq (2):

$$\max D(S, c), D = \frac{1}{|S|} \sum\nolimits_{x_i \epsilon S} I(x_i; c) \tag{2}$$

Here, S represents the set of selected features, while c denotes the class label. Furthermore, to ensure the selection of features with minimal redundancy, a separate formula is applied, structured as Eq (3):

$$\min R(S), D = \frac{1}{|S|^2} \sum\nolimits_{x_i, x_j \epsilon S} I(x_i, x_j) \tag{3}$$

This dual approach underscores the importance of balancing relevance with redundancy minimization in the feature selection process, aiming to optimize the predictive accuracy and interpretability of the model. The mRMR is calculated by Eq (4) as follows:

$$\max \emptyset (D, R), \emptyset = D - R \tag{4}$$

F. PROCESS MULTICHANNEL EEGs

Noise removal, windowing and normalization are among the most important low-level preprocessing methods for EEG signals [3]. EEG signals are susceptible to various types of noise, including electrical interference, muscle activity, and movement artifacts. These noises are commonly removed using different filters, such as band-pass, low-pass, and high-pass, during the low-level preprocessing stage. In this study, we applied these steps according to recommendation of MAHNOB-HCI database [9]. Also, we have used the independent component analysis (ICA) to remove residual noises. Therefore, EEG signals from MAHNOB-HCI were preprocessed as bellow:

1-Band pass Butterworth filter with order 4 and low and high cut frequencies of 1 and 60 Hz and order 4 to remove artefacts

2-Notch filter to remove power line noise

3-Re-reference multichannel EEG signals from MAHNOB-HCI database based on common average method.

4-Downsample signals to 128 Hz to decrease the computational load.

Also, EEG signals from SEED-IV database were passed through all mentioned steps except number 3.

1) DECOMPOSE EEG SIGNALS TO FIVE FREQUENCY BANDS

After these steps, the cleaned EEG signals were decomposed to five frequency bands of delta (1-4 Hz), theta (4-8 Hz), alpha (8-13 Hz), beta (13-25 Hz) and gamma (25-60 Hz) using the discrete wavelet transform (DWT) method with the Daubechies (order 4) mother wavelet at 4 levels [30]. DWT includes two operations as bellow:

1- Filtering: At each level, the signal is split into two parts using high-pass and low-pass filters.

2-Downsampling: After filtering, the signal is downsampled, which means that the number of samples is reduced by half at each level.

FIGURE 3 shows a 30 second EEG signal from SEED-IV database from sad class at the top, then, five frequency bands of delta, theta, alpha, beta and gamma frequency bands are decomposed as mentioned here. Due to downsampling at each level, the length of the resulting signals for each frequency band decreases. For instance, after one level of decomposition, the signal length is halved, after two levels, it is reduced to a quarter of the original length, and so on.

2) EXTRACT FEATURES FROM MULTICHANNEL EEG SIGNALS

Now, four nonlinear entropy features (symbolic dynamic, sample, permutation and phase entropies) are extracted from 62 channels of SEED-IV and 32 channels of MAHNOB-HCI databases at each frequency bands. There features are selected based on efficacy to process nonlinear EEG signals [31], [32], [33]. These features are described at bellow sub-sections.

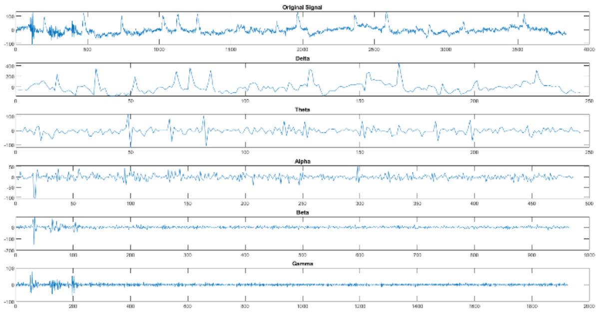

FIGURE 3. An example of a raw EEG signal associated with sadness, showing the delta, theta, alpha, beta, and gamma frequency bands from top to bottom, respectively. The horizontal axis represents the samples, and the vertical axis represents the signal amplitude. The raw signal has a duration of 30 seconds and consists of 3840 samples, given a sampling frequency of 128 Hz.

a: SYMBOLIC DYNAMICS ENTROPY

In the framework of symbolic dynamics, a methodology exists where datasets from the time domain are transmuted into sequences of symbolic representations, facilitating the computation of the probabilities associated with various subsequences as delineated in [33]. This transformation enables the derivation of symbolic dynamics entropy (SymbEn) through the application of Eq (5):

$$SymEn(X, m, \tau, c) = -\sum\nolimits_{a=1}^{c} mp\left(q_a^{c,m,\tau}\right) lnp\left(q_a^{c,m,\tau}\right) - \sum\nolimits_{a=1}^{c} m \sum\nolimits_{b=1}^{c} p\left(q_a^{\varepsilon,m,\tau}\right) lnp\left(q_a^{\varepsilon,m,\tau}\right) .p\left(\sigma_b \mid q_a^{\varepsilon,m\tau}\right) \tag{5}$$

Here, X signifies the series of symbols derived from the time series data, with m representing the embedding dimension, τ indicating the time delay, and ε denoting the alphabet size. The term c^m specifies the total count of distinct states within the system, where a indexes these state patterns (with a ranging from 1 to c^m), and b indexes the individual symbols within the alphabet (with b ranging from 1 to c). The state of the embedding vector is denoted by $q_a^{c,m,\tau}$, while σ_b corresponds to a particular symbol within the alphabet, spanning from 1 to c. In the specific context of calculating SymbEn, parameters are selected as follows: an embedding dimension (m) of 5, a time delay (τ) of 2, and an alphabet size (c) of 3.

b: PHASE ENTROPY

The methodology embodied by phase entropy (PhEn) pertains to the quantitative assessment of signal complexity through an analysis of its representation within the second order difference plot (SODP) [34]. This analytical procedure entails the calculation of the angular inclination for individual data points situated on the SODP and subsequently categorizing the plot into k distinct sectors, with each sector encompassing an angular breadth of $\frac{2\pi}{k}$ radians. This segmentation strategy facilitates the modulation of analysis granularity. The accumulation of slope angles within each designated sector is computed, followed by the derivation of the probability distribution of these slope angles across the sectors, denoted as $p(i)$. Utilizing this probability distribution, the Shannon entropy, referred to as PhasEn, is then calculated, as indicated in reference. This entropy serves as a metric for the signal's complexity by quantifying the diversity in its phase space distribution as represented on the SODP [34].

$$PhasEn = -\frac{1}{\log k} \sum\nolimits_{i=1}^{k} p(i) \, logp(i) \tag{6}$$

where, k is set 5.

c: PERMUTATION ENTROPY

Permutation entropy (PermEn) is a metric for evaluating the prevalence of ordinal patterns within a time series dataset by constructing a multidimensional sequence vector, which is contingent upon the parameters of embedding dimension and time delay, analogous to methodologies employed by approximate entropy and SampEn [35]. This involves the generation of a multidimensional sequence vector through the specification of an embedding dimension, denoted as m, and a time delay, denoted as τ. The formal expression for PermEn, is calculated by Eq.(7) as follows [35]:

$$PermEn = -\sum\nolimits_{i}^{m!} p_i \ln p_i \tag{7}$$

In this context, p_i represents the probability of encountering each specific pattern within the dataset, and m signifies the embedding dimension. For the purposes of the conducted analysis, the parameters were established with $m = 5$, indicating an embedding dimension, and the time delay, τ, was set to 2. Sample entropy (SampEn) SampEnis a statistical measure employed for assessing the likelihood that two subsequences, differing by one in their length (m and $m+1$), will remain similar to each other within a specified tolerance (r). This index effectively measures the self-similarity of a time series, as articulated in Eq.(8) [36]:

$$SampEn(m, r, N) = -\ln\left[\frac{\sum_{i=1}^{n-m\tau} A_i}{\sum_{i=1}^{n-m\tau} B_i}\right] \tag{8}$$

In this equation, A_i denotes the count of pairs of sequences that match within a tolerance r in the $(m+1)$-dimensional space, whereas B_i signifies the count of matching pairs in the m -dimensional space. Here, X_i elements are compared within a tolerance r of X_j, with these elements forming part of either the m -dimensional or $(m+1)$-dimensional pattern vectors, as indicated in [37]. For the purpose of calculating this form of entropy, parameters are set with $m = 5$ as the embedding dimension, $\tau = 2$ as the time delay, and r as 0.15 times the standard deviation of the time series signal, thereby providing a standardized approach to quantify temporal regularity and predictability within the dataset.

G. FUZZY LOGIC

In a general statement, it is said that the complexity of the universe comes from its uncertainty, where humans are able to understand ambiguities and complications due to the power

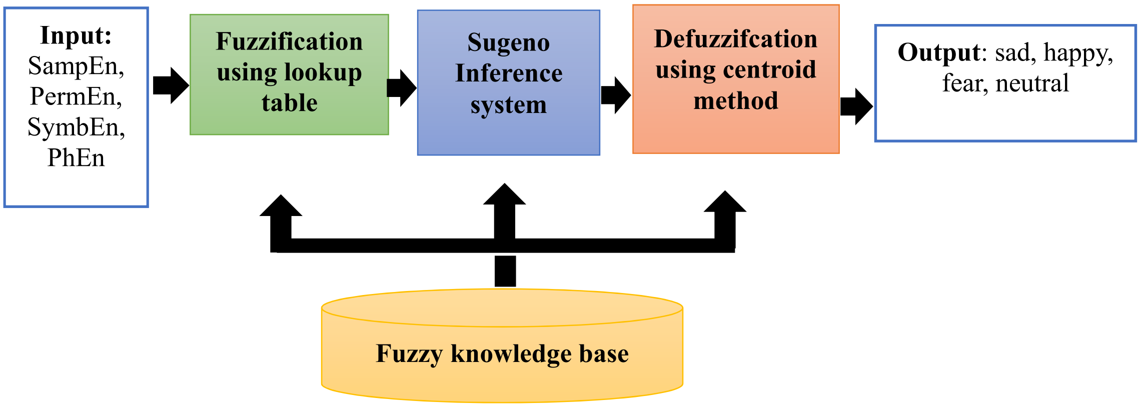

FIGURE 4. Flowchart of our proposed S-FIS of ER system.

of thinking. Many real-world problems cannot be solved by classical set theory, in classical set theory an element or member of the set is or is not, or zero or one. The opposite point of classical set theory is fuzzy theory [38], [39]. We are faced with uncertainty in the phenomenon of ER, whether a system can identify exactly one type of emotion or what knowledge an expert has to recognize emotions, fuzzy set theory is a powerful tool to deal with the uncertainty of emotion expression due to ambiguity. Although fuzzy systems describe uncertain and uncertain phenomena, the fuzzy theory itself leads to a precise theory.

1) S-FIS METHOD

FIGURE 4 shows the architecture of the S-FIS for fuzzing emotional signals. As it is known, the FIS is generally made of three components of fuzzifier, fuzzy inference engine and defuzzifier. The process of converting explicit variables into linguistic variables is called fuzzification which in this study we have used lookup table method [40], [41]. By performing various steps, selected features over all samples are given as input to the S-FIS [42], and these inputs are the same features that are divided into 5 folders, and each time 4 folders are discretized in 2, 3, and then in 4 levels and given to this section, and pruning rules are obtained in the final stage using the GA [43], [44]. Also, each time a remaining category is given to the same fuzzy classifier for testing. The inference engine evaluates and infers the rules using inference algorithms, and after collecting the output rules, it is converted into an explicit or numerical value by the de-fuzzifier unit. In this study we have used the centroid method [45] to defuzzify triangular membership functions. Centroid defuzzification calculates the center of gravity for the fuzzy set along the x-axis. Imagine the area as a uniformly thick and dense plate; the centroid represents the point on the x-axis where the fuzzy set would achieve equilibrium. Simply put, the fuzzy inference engine here expresses a knowledge base for rule extraction from the ER system.

One point is choosing the number of membership functions, which is based on the expert decision which determines it according to the type of system and her/ his personal knowledge and experience. It should not be noticed that the number of membership functions should be justified, that is, not so low that the designed fuzzy system has poor performance and high error, and not so much that the system calculations increase due to the increase in the number of rules and the designed system becomes expensive. However, in some cases, due to the complexity of the system, high resolution is required, so the number of membership functions should be increased. The number of membership functions in this study are 2, 3 and 4. Then, these membership function can be considered in different shapes, such as triangular, Gaussian and etc. Triangular membership function is used in this study, then, split points of concepts (features) were discretized using the entropy method. FIGURE 5 shows a triangular membership function for PhEn-FP2 and three conceptual levels of 'Low', 'Medium' and 'High'. Then, fuzzy rules (fuzzy operators) are determined from EEG features that were selected from mm method. These rules are usually defined based on the following model:

IF variable is set, **THEN** action

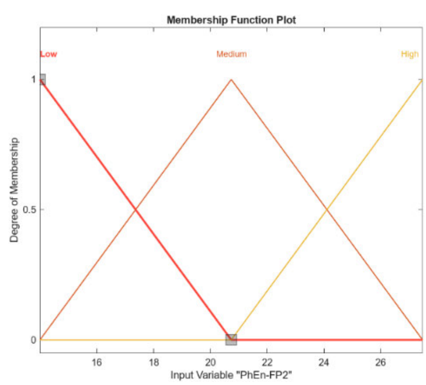

FIGURE 5. Triangular membership functions for the PhEn feature of FP2 channel. This feature was discretized into three conceptual levels of 'Low', 'Medium' and 'High'.

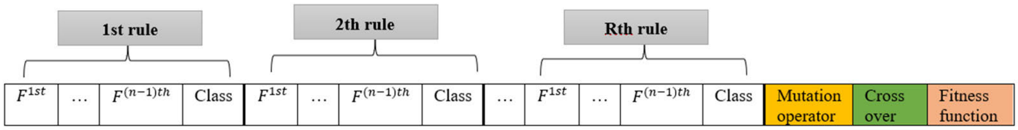

FIGURE 6. Structure of our proposed chromosome in GA.

2) OPTIMIZING RULES USING GA

Up to this point, a fuzzy rule has been obtained for all rows of the database (features). In this step, to further refine the rules and further simplify the fuzzy system, another step is performed on all the rules of the dataset rows:

If there are conflicting rules, i.e., rules that have the same front part (If) and different tail (Then), only one rule is selected with a greater weight. This work has been done by obtaining the parameters related to the membership functions and then calculating their probability, and finally the rules that have the highest probability are selected. For example, a rule that says that if the value of entropy feature in beta band is low then it leads to a class event of sadness and another rule with a different antecedent and sadness again, pruning should be started and to the rule that gets more points should be attributed. Of course, in this study, in order not to lose the extractive knowledge of strong and inconsistent rules with high degree of belonging, and to make better decisions, the S-FIS-GA has been trusted.

As mentioned before, one of the most important parts of this study is creating a reliable knowledge base to identify emotions. In the previous section, it was explained how the basic rules are made, and these rules are entered in the GA cycle for optimization during a proposed algorithm, and the rules are optimized. In the implementation of the GA, it is important to answer two questions: 1) How should the initial chromosomes be? 2) How should the optimization function work? In response to the initial question, the decision was made to rely on the algorithm for extracting the initial rules of emotions, during which the identified initial compatible rules were considered as primary chromosomes, and then to select the optimization function to extract better rules in the next generations, two points It was considered: one is to increase the accuracy of the classification and the other is to cover the knowledge base extracted from the set of rules. Taking into account the stated assumptions of other parameters of the GA, we have proceeded selectively, which will be explained bellow.

In fact, fuzzy system design is done in two stages, 1- preliminary design and 2- knowledge extraction with lookup table algorithm. In the next step, the GA is used to tune S-FIS rules. Note that, in both steps of design, the output of the knowledge expressed is in the recognition of emotions. In the first step, this knowledge is limited to scoring based on the membership functions of the features, and in fact, with lookup table, this knowledge leads to if-then rules for the class output of emotions, and in the next step, after the initial pruning and removing the inconsistent rules, during the optimization steps, best rules are selected for the design of the conceptual rule system. The proposed chromosome structure for GA is shown in FIGURE 6.

H. EVALUATION CRITERION

K-fold CV is used to evaluate the proposed S-FIS-GA-ER method with K=5. Three best features of SampEn-T8, PermEn-T7 and PhaEn-FP2 for all subjects are divided into five folds, four folds are used to train FIS and one-fold for test. This procedure is repeated five times. Average of accuracy, true positive rate (TPR), false negative rate (FNR) and area under the curve (AUC) are calculated for each fold by Eq (9)-(12) [46]. Where, tp_i is true positive for class i, tn_i is true negative for class i, fp_i is false positive for class i, and fn_i is false negative for class i. (AUC is calculated as a binary problem).

$$Accuracy = \frac{\sum_{i=1}^{l} \frac{tp_i+tn_i}{tp_i+tn_i+fp_i+fn_i}}{l} \tag{9}$$

$$TPR = \frac{\sum_{i=1}^{l} \frac{tp_i}{tp_i+fn_i}}{l} \tag{10}$$

$$\mathrm{FNR} = \frac{\sum_{i=1}^{l} \frac{fn_i}{tp_i+fn_i}}{l} \tag{11}$$

$$AUC = \frac{1}{2}\left(\frac{tp}{tp+fn} + \frac{tn}{tn+fp}\right) \tag{12}$$

IV. RESULTS

A. EYE TRACKER

In the first step, eye track data for both databases are monitored and segmented into lower parts to extract desired features. These features include average and standard deviation of fixation duration, fixation frequency and maximum fixation duration, average and standard deviation of pupil diameter in X and Y directions, respectively, [7]. Finally, these 8 features are extracted from every 4 second segments, length of segments are selected according to [7]. FIGURE 7 shows results of the mRMR feature selection method for the SEED-IV (a) and MAHNOB-HCI (b) databases. In this figure, the features are ranked from highest to lowest as follows: average pupil diameter in the Y direction, average pupil diameter in the X direction, average fixation duration, standard deviation of pupil diameter in the Y and X directions, fixation frequency, maximum fixation duration, and standard deviation of fixation duration. As it can be observed,

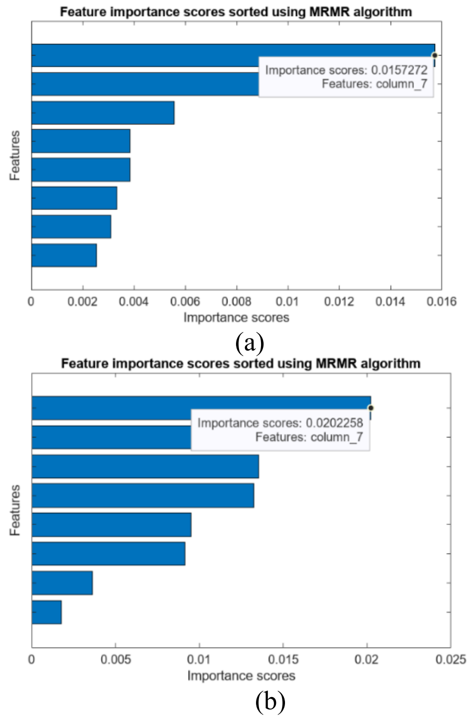

FIGURE 7. Results of mRMR method to rank features ascending for the SEED-IV (a) and MAHNOB-HCI (b) databases. Seventh feature (average of pupil diameter in Y direction) achieved highest rank among others. The features are ranked from highest to lowest as follows: average pupil diameter in the Y direction, average pupil diameter in the X direction, average fixation duration, standard deviation of pupil diameter in the Y and X directions, fixation frequency, maximum fixation duration, and standard deviation of fixation duration.

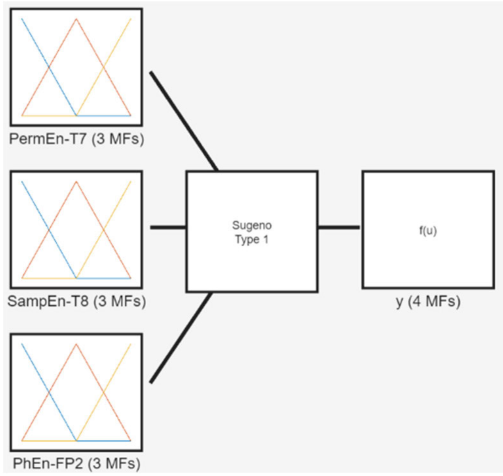

FIGURE 8. The proposed S-FIS based on lookup table algorithm with 3 input and 27 rules. Each input has three levels of low, medium and high. Triangular membership functions are considered for three selected features (input) of PermEn from T7 channel, SampEn from T8 channel and PhaseEn from Fp2 channel. These features were selected using mRMR method for SEED-IV database.

this feature can be effectively distinguishing four emotional classes for both databases.

Then, this feature is used in gate strategy to determine an event, in the other hand, in this strategy, parts of signals after this event was selected. The maximum of this feature is calculated and used as threshold, i.e., eye track is monitored and each time this feature reached the maximum values, that moments were marked and time in EEG signal were used for analysis.

B. EEG SIGNALS

After pre-process step, multichannel EEG signals from each database are segmented into 4 seconds. Then, four features of SampEn, PermEn, SymbEn and PhEn were extracted from each segment of 62 and 32 channels from SEED-IV and MAHNOB-HCI databases, respectively. Finally, 248 and 128 features from these channels are computed. Then, three common features among five frequency bands and channels from selection of mRMR method are used. These features are PhEn, SampEn and PermEn for T7, T8 and Fp2 channels of both databases, respectively. These features are used as input of S-FIS (FIGURE 8). As said earlier, the FIS is created using lookup table algorithm. The mentioned features are discretized into two, three and four levels using the entropy criterion. Finally, three levels had higher performance based on average accuracy value among four emotional categories. Also, the membership functions were set triangular. Finally, 27 (3 membership function for PhEn-T7 $\times 3$ membership function SampEn-T8 $\times$ 3 membership function PermEn-Fp2) rules are created for each frequency bands. These FIS are tuned using the GA.

Population size is based on number of membership functions equal to 27 (3 membership function for SampEn $\times 3$ membership function for PermEn $\times$ 3 membership function for PhEn). Also, fitness function is according to the coverage of rules among samples and the accuracy. After creating rules, accuracy is calculated to investigate strength of rules. Notice that, a rule can have high accuracy but not coverage, therefore we have considered the coverage as the second metric. Coverage means how many rules are fired by samples, in other words, after creating rules, features are scanned and rules with higher coverage win.

FIGURE 9 shows results of tuning fuzzy rules of alpha frequency band for SEED-IV database using the GA. This process stops after 450 generation due to no change in fitness value in the last 10 steps. The speed of running the algorithm is not very important here because the use of knowledge extracted only leads to the creation of a platform for use in the field of ER.

In total, a set of 10 rules has been extracted for each sub-band of brain signals. The rules are arranged according to their importance, for example, the first rule for delta frequency band is more important than the second rule. But the most important rule for detection of happiness is rule number seven. Therefore, in total, according to the existence of 5 frequency bands and the presence of the top 10 rules in each sub-band, a total of 50 rules have been identified. In the following, for each band, a rule package of 4 of the best discriminative rules for 4 emotional classes is presented.

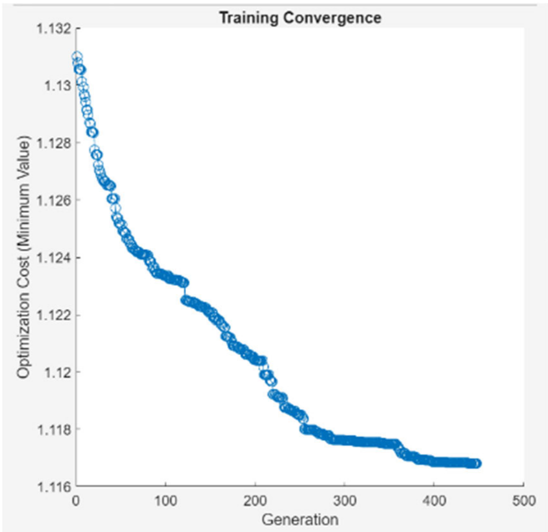

FIGURE 9. Training curve resultant from tuning fuzzy rules of alpha frequency band for SEED-IV database using the GA. This process is stopped after 450 generation. Stopping criterion was no further proceeding of fitness value after 10 generation.

TABLE 2. Set A: 10 top fuzzy rules for delta frequency band from the SEED-IV database.

If	Then
1-If PhEn-FP2 is medium and SampEn-T8 is medium and PermEn-T7 is high	class is neutral
2-If PhEn-FP2 is medium and SampEn-T8 is low and PermEn-T7 is medium	class is sad
3-If PhEn-FP2 is medium and SampEn-T8 is high	class is neutral
4-If PhEn-FP2 is low and PermEn-T7 is low	class is sad
5-If PhEn-FP2 is medium and SampEn-T8 is medium and PermEn-T7 is medium	class is neutral
6-If PhEn-FP2 is low and SampEn-T8 is medium and PermEn-T7 is medium	class is fear
7-If PhEn-FP2 is high and PermEn-T7 is high	class is happy
8-If SampEn-T8 is high and PermEn-T7 is high	class is sad
9-If PhEn-FP2 is low and SampEn-T8 is high	class is sad
10-If SampEn-T8 is medium	class is happy

According to TABLE 2, for the delta band, rule number 1 is chosen to detect the neutrality, rule number 2 is chosen to detect the feeling of sadness, rule number 6 is chosen to detect the feeling of fear, rule number 7 is chosen for the feeling of happiness. Also, the results of this set state that the SampEn of the T8 channel plays a good role in expressing the feeling of happiness.

According to TABLE 3, rules for the theta band, in order to detect the feeling of neutrality, rule number 3 was chosen to detect the feeling of sadness. No rule was chosen to detect the feeling of fear (in other words, the feeling of fear was not seen in the theta band). Also, rule number 4 was chosen for feeling happy. In addition, the results of this group state that the entropy of the T8 channel plays a good role in expressing the sense of neutrality.

TABLE 3. Set B: 10 top fuzzy rules for theta frequency band from the SEED-IV database.

If	Then
1-If PhEn-FP2 is medium and SampEn-T8 is medium	class is sad
2-If PhEn-FP2 is medium and SampEn-T8 is low and PermEn-T7 is low	class is sad
3-If PhEn-FP2 is medium and SampEn-T8 is high and PermEn-T7 is medium	class is neutral
4-If PhEn-FP2 is medium and SampEn-T8 is low and PermEn-T7 is high	class is happy
5-If PhEn-FP2 is low and PermEn-T7 is high	class is neutral
6-If PhEn-FP2 is low and SampEn-T8 is high and PermEn-T7 is low	class is neutral
7-If PhEn-FP2 is medium and PermEn-T7 is medium	class is happy
8-If SampEn-T8 is high	class is neutral
9-If PhEn-FP2 is medium and SampEn-T8 is medium and PermEn-T7 is medium	class is happy
10-If PhEn-FP2 is high and SampEn-T8 is low and PermEn-T7 is medium	class is neutral

TABLE 4. Set C: 10 top fuzzy rules for alpha frequency band from the SEED-IV database.

If	Then
1-If PhEn-FP2 is high and SampEn-T8 is medium and PermEn-T7 is low	class is happy
2-If PhEn-FP2 is low and PermEn-T7 is high	class is happy
3-If PhEn-FP2 is medium and SampEn-T8 is medium and PermEn-T7 is medium	class is fear
4-If PhEn-FP2 is medium and SampEn-T8 is medium and PermEn-T7 is low	class is happy
5-If PhEn-FP2 is low and SampEn-T8 is low and PermEn-T7 is medium	class is sad
6-If PhEn-FP2 is medium and SampEn-T8 is high and PermEn-T7 is low	class is fear
7-If PhEn-FP2 is low and SampEn-T8 is medium and PermEn-T7 is medium	class is happy
8-If PhEn-FP2 is medium and SampEn-T8 is medium	class is sad
9-If PhEn-FP2 is high and PermEn-T7 is medium	class is fear
10-If PhEn-FP2 is low and SampEn-T8 is medium and PermEn-T7 is low	class is neutral

According to TABLE 4 for alpha band, rule number 10 was chosen to detect the feeling of neutrality, rule number 5 was chosen to detect the feeling of sadness, rule number 3 was chosen to detect the feeling of fear, and rule number 1 was chosen for the feeling of happiness.

Results of rules for beta frequency (set D) in TABLE 5 are approximately similar to set C for alpha frequency band. For example, rule number 10,5,3 and 1 were chosen to detect the feelings of neutrality, sadness, fear and happiness, respectively.

According to TABLE 6, rules for the gamma band, rule number 10 was chosen to detect the feeling of neutrality, rule number 5 was chosen to detect the feeling of sadness,

TABLE 5. Set D: 10 top fuzzy rules for beta frequency band from the SEED-IV database.

If	Then
1-If PhEn-FP2 is high and SampEn-T8 is medium and PermEn-T7 is low	class is happy
2-If PhEn-FP2 is low and PermEn-T7 is high then	class is happy
3-If PhEn-FP2 is medium and SampEn-T8 is medium and PermEn-T7 is medium	class is fear
4-If PhEn-FP2 is medium and SampEn-T8 is medium and PermEn-T7 is low	class is happy
5-If PhEn-FP2 is low and SampEn-T8 is low and PermEn-T7 is medium	class is sad
6-If PhEn-FP2 is medium and SampEn-T8 is high and PermEn-T7 is low	class is fear
7-If PhEn-FP2 is low and SampEn-T8 is medium and PermEn-T7 is medium then	class is happy
8-If PhEn-FP2 is medium and SampEn-T8 is medium	class is sad
9-If PhEn-FP2 is high and SampEn-T8 is low and PermEn-T7 is medium	class is fear
10-If PhEn-FP2 is low and SampEn-T8 is medium and PermEn-T7 is low	class is neutral

TABLE 6. Set E: 10 top fuzzy rules for gamma frequency band from the SEED-IV database.

If	Then
1-If PhEn-FP2 is low and Perm-FP2 is high	class is happy
2-If PhEn-FP2 is high and SampEn-T8 is medium and PermEn-T7 is low	class is happy
3-If PhEn-FP2 is medium and SampEn-T8 is medium and PermEn-T7 is medium	class is fear
4-If PhEn-FP2 is medium and SampEn-T8 is medium and PermEn-T7 is low	class is happy
5-If PhEn-FP2 is low and SampEn-T8 is low and PermEn-T7 is medium	class is sad
6-If PhEn-FP2 is medium and SampEn-T8 is high and PermEn-T7 is low	class is fear
7-If PhEn-FP2 is low and SampEn-T8 is medium and PermEn-T7 is medium	class is happy
8-If PhEn-FP2 is medium and SampEn-T8 is medium	class is sad
9-If PhEn-FP2 is low and SampEn-T8 is medium and PermEn-T7 is low	class is neutral
10-If PhEn-FP2 is high and SampEn-T8 is low and PermEn-T7 is high	class is fear

rule number 6 was chosen to detect the feeling of fear, rule number 1 was chosen for the feeling of happiness.

Overall, for all frequency bands, the medium concept of PhEn have a significant role in ER.

FIGURE 10 illustrates confusion matrix of our S-FIS-GA-ER for recognition of four emotional categories of (1) sadness, (2) happiness, (3) fear and (4) neutrality for five frequency bands for the SEED-IV database for the best fold. Alpha frequency band achieves the highest average accuracy of 94.42% for four mentioned classes. Then, beta and gamma frequency bands achieved the average accuracies of 93.02% and 89.80%. Both theta and delta frequency bands achieved lower accuracies.

As it can be observed from FIGURE11, values of AUC for each frequency bands and classes are higher than 0.9 which demonstrate the efficacy of our proposed S-FIS-GA-ER method for the SEED-IV database. All of the frequency bands have excellent rules that achieved highest performance to recognize sadness (1), happiness (2), fear (3) and neutral (4) for this database, respectively. The alpha and beta frequency bands achieved the highest AUC values approximately 0.99 for each class. Then, gamma, theta and delta achieve the AUC values of approximately 0.98, 0.95 and 0.90, respectively.

As mentioned earlier, our proposed S-FIS-GA-ER system is adaptive, so, we did not design a distinct rule base for MAHNOB-HCI database. Rule base of SEED-IV database is tuned using the MAHNOB-HCI database. FIGURE 12 illustrates confusion matrix of our S-FIS-GA-ER for recognition of four emotional categories of (1) sadness, (2) happiness, (3) fear and (4) neutral for five frequency bands for the MAHNOB-HCI database for the best fold. Alpha frequency band achieves the highest average accuracy of 85.2% for four mentioned classes. Then, beta and gamma frequency bands achieved the average accuracies of 82.92% and 79.05%. Both theta and delta frequency bands achieved lower accuracies.

As it can be observed from FIGURE 13, values of AUC for each frequency bands and classes are higher than 0.9 which demonstrate the efficacy of our proposed S-FIS-GA-ER method for the MAHNOB-HCI database. All of the frequency bands have excellent rules that achieved highest performance to recognize sadness (1), happiness (2), fear (3) and neutral (4) for this database, respectively. The alpha and theta frequency bands achieved the highest AUC values approximately 0.97 for each class. Then, beta, gamma and delt achieves the AUC values of approximately 0.95, 0.94 and 0.93, respectively.

V. DISCUSSION

In this study, an interesting idea is investigated to improve performance of ER systems from multimodal emotional databases. We have proposed an eye-gated strategy to improve performance of ER system based on multichannel EEG signals. To do this, we have used two multimodal emotional databases, the eye-track data is used to find effective parts for each subject and after that, the corresponding EEG signals are processed. As our knowledge, this idea is for the first time to be investigated in ER area from these modalities. Indeed, our hypothesis was that when a person watches an emotional clip as stimulation, some features resulted from the eye-track can be useful to correspond with effective parts of EEG signal. For example, during watching a thriller, fixation duration or pupil diameter in x direction decrease, or during happiness these features increases. So, we have considered this information to increase accuracy of ER system.

A. EYE TRACK DATA AND EMOTION

According to FIGURE 7 (a) and (b), average of pupil diameter in Y direction has been chosen as best feature among 8 features using the mRMR method. This feature is used as the candid for selecting effective parts from EEG signals. Scientific studies have further elucidated the

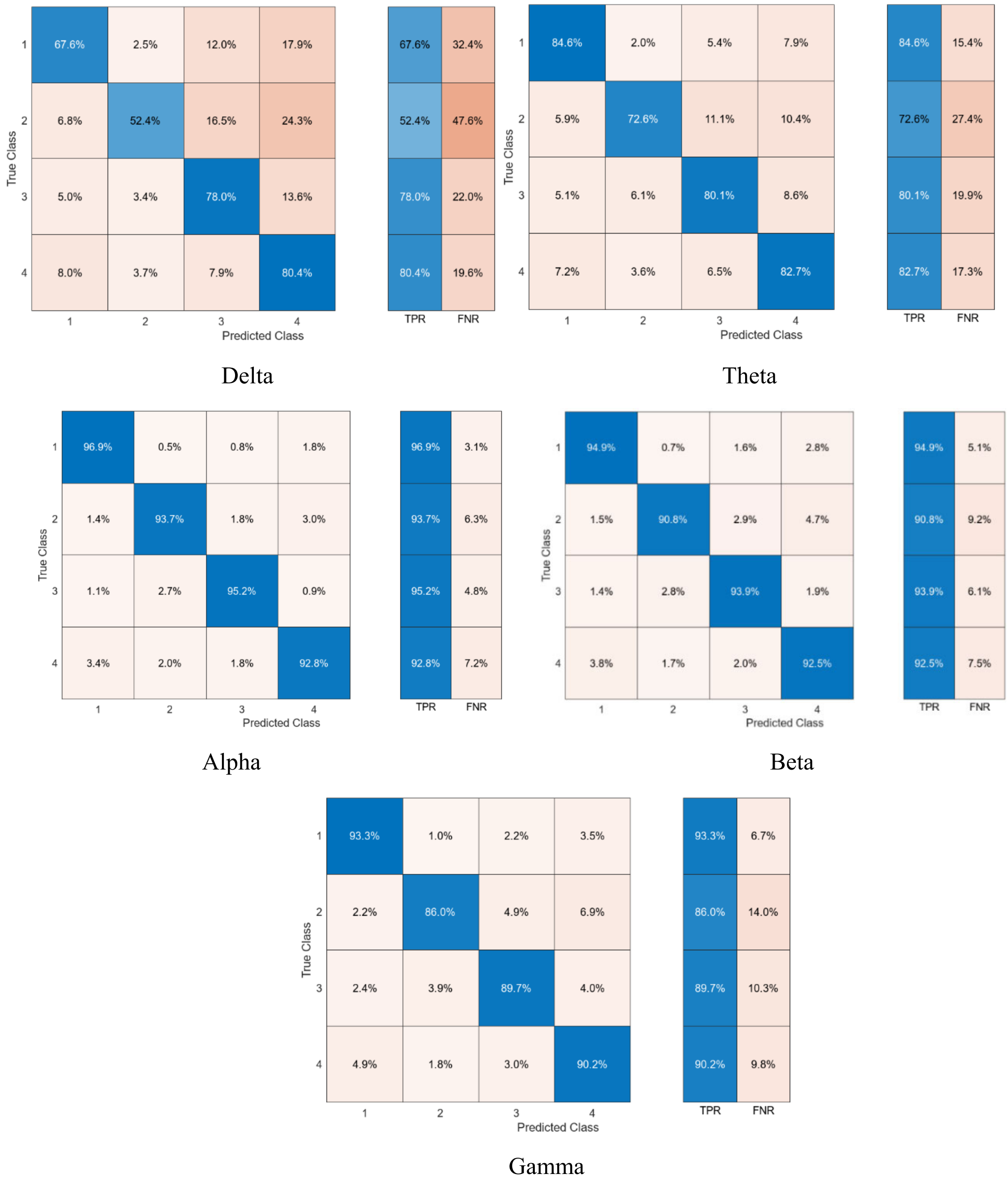

FIGURE 10. **Confusion matrix of our proposed S-FIS-GA-ER for five frequency bands on the SEED-IV database. Values of 1 to 4 for each confusion matrix stands for sadness, happiness, fear and neutrality, respectively.**

intricate relationship between pupil diameter and emotions, shedding light on the physiological underpinnings of emotional responses. One such study explored how pupil dilation reflects the time course of ER in human vocalizations, demonstrating that pupil dilation is significantly influenced by emotional intensity, sound duration, and the ambiguity of the stimuli. The research found that pupil size increased more vigorously in response to auditory stimuli of higher emotional intensity and longer duration. This variation in pupil response, although relatively subtle compared to the impact of baseline pupil size, was highly significant and highlighted the independent contributions of cognitive load (e.g., response time) and affective processing (e.g., valence intensity) to pupil dilation [47]. Another study focused on the physiological responses to awe experiences, employing a within-subjects design to manipulate emotions through video clips that induced feelings of awe, amusement, or were neutral. This research aimed to understand how awe and other emotional states affect physiological measures, including pupil diameter. While the study's primary focus was on

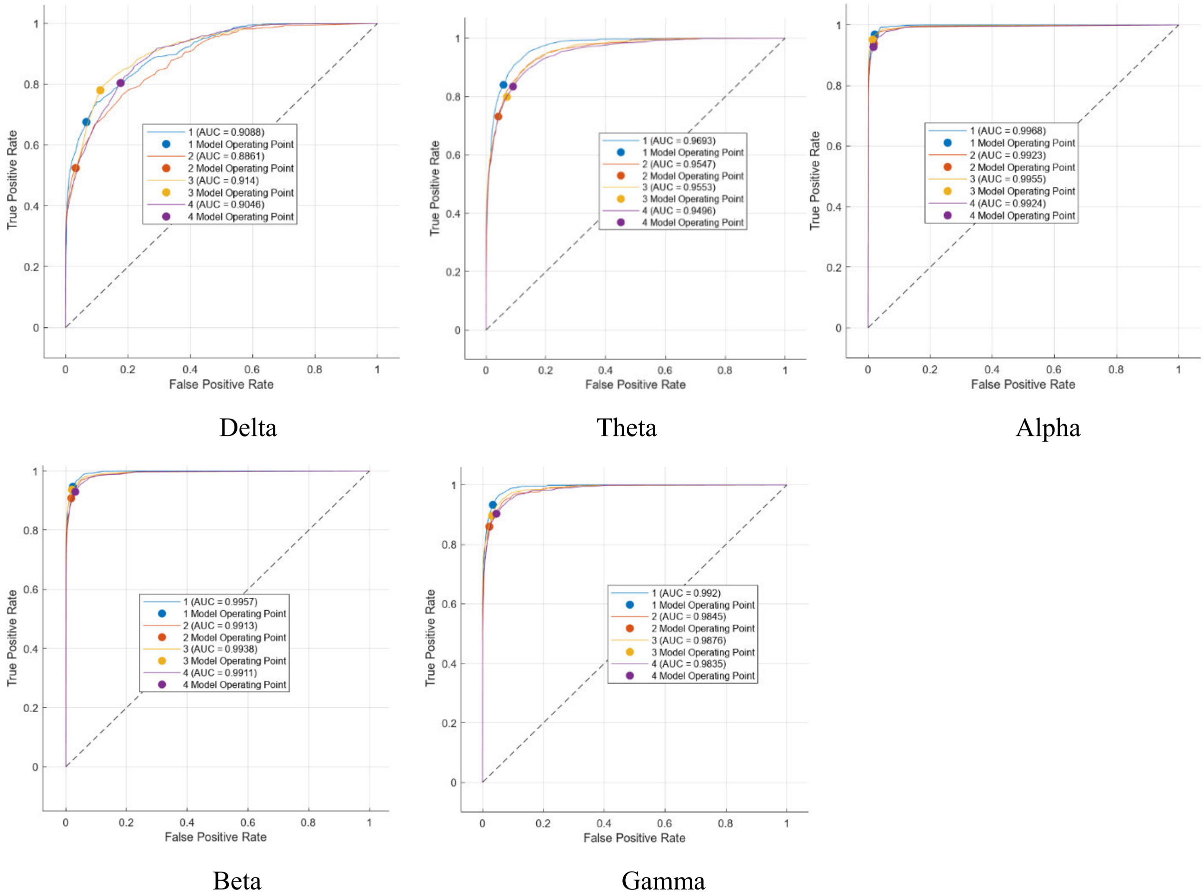

FIGURE 11. ROC curves for five frequency band corresponding to the proposed S-FIS-GA-ER for SEED-IV database. Values of 1 to 4 for each confusion matrix stands for sadness, happiness, fear and neutrality, respectively.

awe experiences, it contributed to the broader understanding of how various emotional states can influence physiological responses, emphasizing the complex interplay between emotional experiences and physical reactions [48]. These findings underscore the multifaceted nature of the relationship between pupil diameter and emotions, indicating that both the intensity of emotional stimuli and cognitive factors related to processing these stimuli play significant roles in modulating pupil size. The results from these studies not only confirm the connection between pupil dilation and emotional arousal but also highlight the importance of considering both affective and cognitive dimensions when interpreting pupillometric data in emotional research.

B. RELATION BETWEEN EYE TRACK, EEG AND EMOTION

The relationship between eye-tracking data and EEG signals is a subject of increasing interest in neuroscience, psychology, and human-computer interaction studies. Eye-tracking measures where and when a person's gaze occurs, while EEG records electrical activity in the brain. These two methods, when combined, can offer comprehensive insights into human cognition [49], attention [50], neurological processes [51] and emotion recognition [7]. Duchowski [49] has shown that integrating eye-tracking with EEG data can provide a more nuanced understanding of cognitive load. For instance, eye metrics such as blink rate, saccades, and fixations, when analyzed alongside EEG signals, particularly in the frontal lobe, can indicate levels of engagement, mental effort, and fatigue. In another study, Polich [50] investigate relation between both eye-tracking and EEG data in attention and information processing. The P300 wave in EEG signals, which reflects attentional processes and memory updating, can be temporally correlated with eye movement events to infer how attention is allocated in tasks requiring visual search. This combination helps in deciphering how visual attention mechanisms are linked with cognitive processes. The concurrent use of EEG and eye-tracking has also been applied in the diagnosis and study of neurological and psychological disorders. For example, abnormalities in eye movement patterns, when combined with specific EEG patterns, can help in the early detection of disorders such as ADHD, autism, and schizophrenia [51]. This multidimensional approach allows for a better understanding of the disorders' underlying cognitive and neural mechanisms. In the field of human-computer interaction, combining eye- tracking and EEG data helps in designing more effective user interfaces. For instance, understanding how users allocate their visual attention and cognitive resources while

IEEE Access

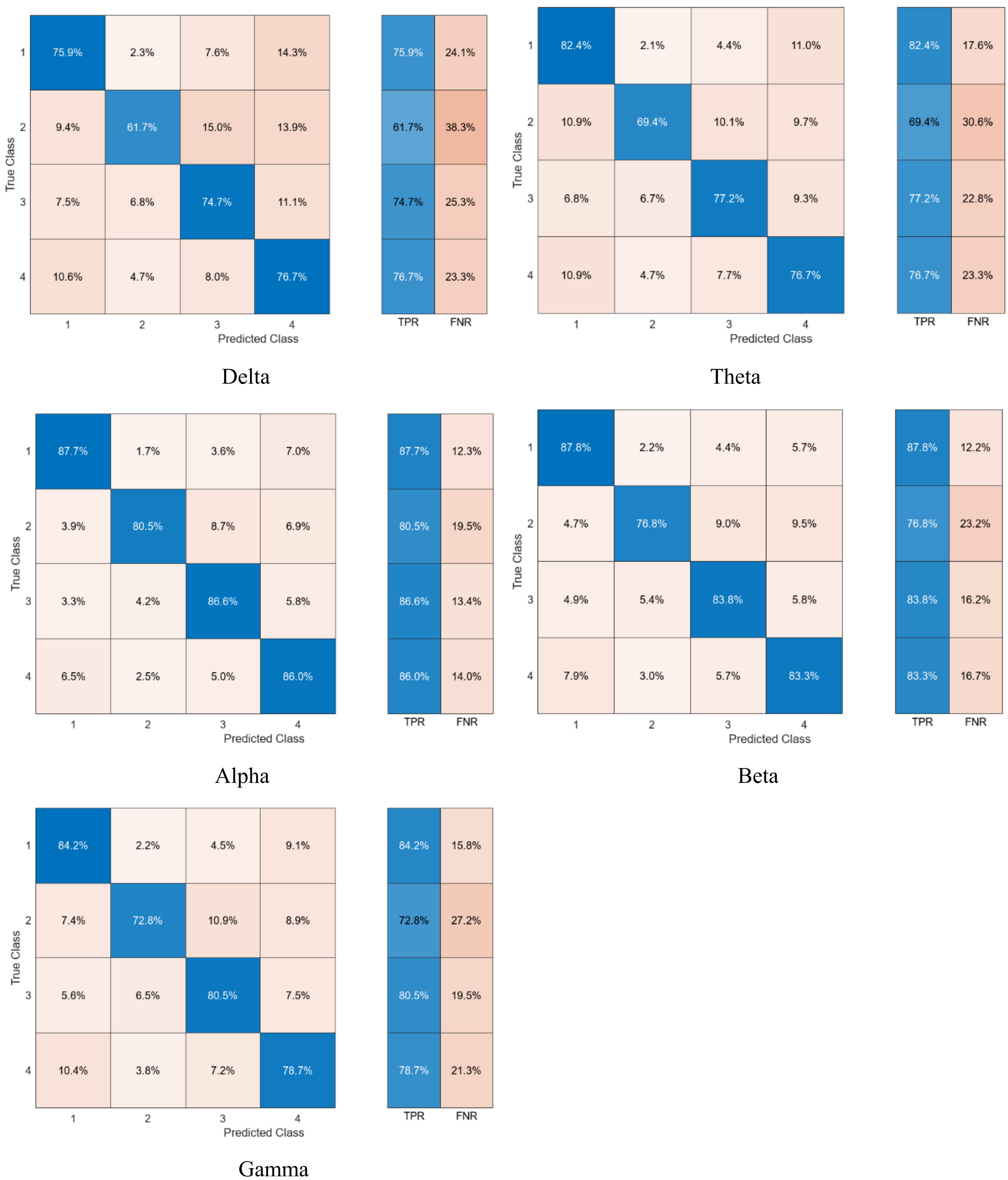

FIGURE 12. Confusion matrix of our proposed S-FIS-GA-ER for five frequency bands on the MAHNOB-HCI database. Values of 1 to 4 for each confusion matrix stands for sadness, happiness, fear and neutral, respectively.

interacting with interfaces can inform more accessible and user-friendly designs [52]. These examples illustrate the broad and impactful applications of combining eye-tracking and EEG data across various fields. The integration of these methods continues to provide valuable insights into human cognition, behavior, and interaction with technology. However, it is important to acknowledge the complexity of simultaneously collecting and analyzing these data types. Rigorous methodological approaches and advanced analytical techniques are required to effectively interpret the multimodal data generated from these sources.

Zheng et al. [7] present EmotionMeter, a multimodal emotion recognition framework that combines brain waves and eye movements. They demonstrate that fusing EEG and

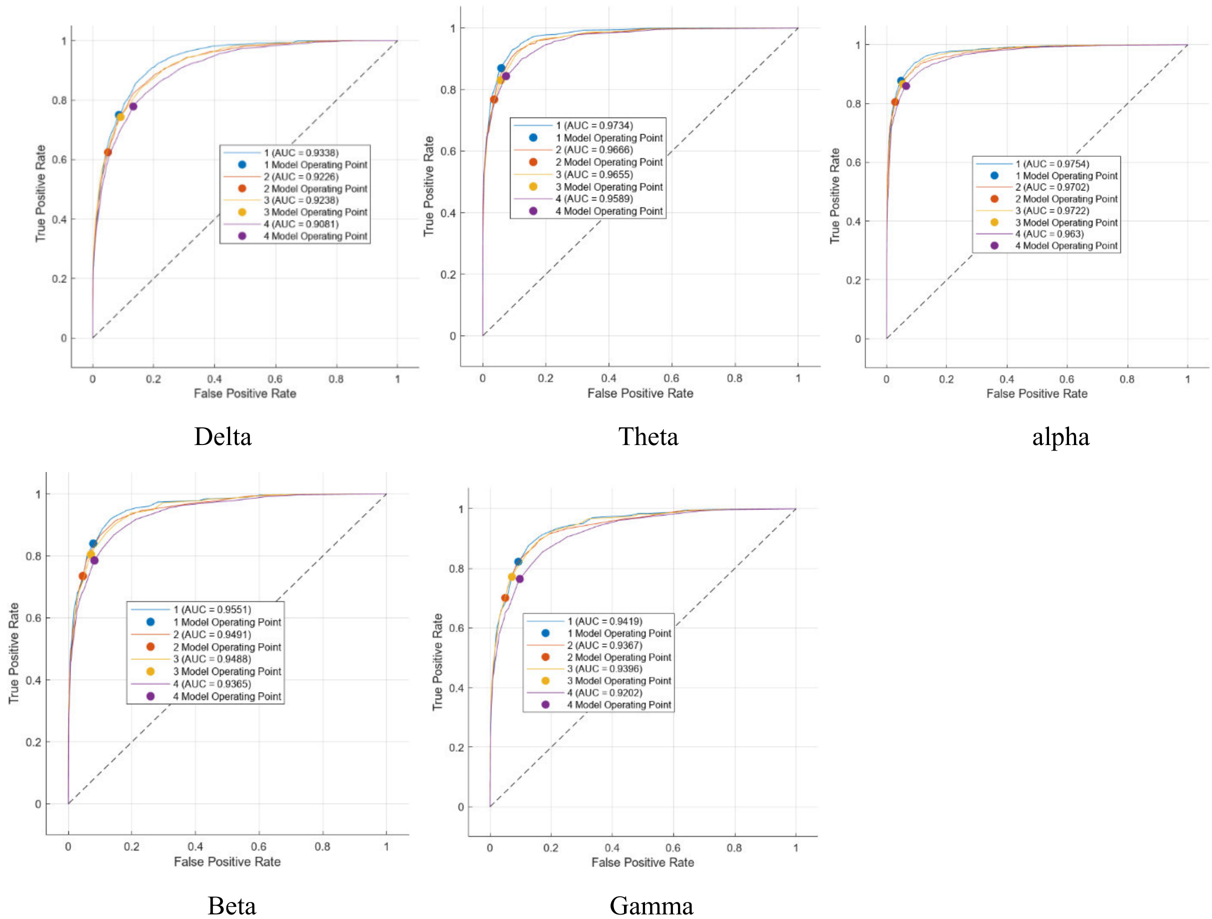

FIGURE 13. ROC curves for five frequency band corresponding to the proposed S-FIS-GA-ER for MAHNOB-HCI database. Values of 1 to 4 for each confusion matrix stands for sadness, happiness, fear and neutrality, respectively.

eye movements with multimodal deep learning significantly enhances emotion recognition accuracy (85.11%) compared to using a single modality (eye movements: 67.82%, EEG: 70.33%).

All of these works used EEG and eye-tracking data separately. But in this study, we used eye-track data as gated strategy to select effective parts of EEG signals related to emotions.

C. FREQUENCY BANDS AND SELECTED CHANNELS

According to FIGURE 10 to FIGURE 13, alpha, beta and gamma frequency bands are more prominent in discriminating mentioned emotional categories. Results for these frequency bands are consistent with [7], [53], [54], [55], and [56]. The research has consistently identified the alpha, beta, and gamma frequency bands as key neural correlates of emotion, highlighting their significant relationship with emotional processes. Moreover, numerous psychological investigations have delved into the specific role of the alpha frequency band in relation to emotional states. These studies collectively reveal that the alpha band stands out for its crucial role in the processing of emotions, suggesting its predominance in the emotional response system.

According to the results, the two temporal EEG channels, T7 and T8, achieved the highest accuracies. Physiological research indicates that the temporal lobe is related to emotions. The brain is divided into three main anatomical sections: the hindbrain, midbrain, and forebrain. The cerebrum, part of the forebrain, is further divided into two hemispheres. The outer layer of the cerebrum, known as the cerebral cortex, consists of four major lobes: the frontal, occipital, parietal, and temporal lobes. The amygdala is located within the temporal lobe, specifically in the medial temporal lobe near the hippocampus. It is an almond-shaped cluster of nuclei deeply involved in processing emotions, particularly fear and pleasure, as well as in forming emotional memories. The relationship between the amygdala and the temporal lobe is significant because the temporal lobe plays a crucial role in integrating sensory input with emotional responses, memory formation, and processing. The close proximity and interaction between the amygdala and the hippocampus within the temporal lobe are vital for the integration of emotional experiences with memory, influencing how

TABLE 7. Selected Rules for both databases resultant from five frequency bands for each emotional category.

Rule for sadness	Coverage	Accuracy
If PhEn-FP2 is medium and SampEn-T8 is low and PermEn-T7 is medium	57%	75.78%
If PhEn-FP2 is low and SampEn-T8 is low and PermEn-T7 is medium	44%	73.90%
If phT7 Is medium, sampT8 Medium	43%	72.45%

Rule for happiness	Coverage	Accuracy
If PhEn-FP2 is high and PermEn-T7 is high	58%	82.65%
If PhEn-FP2 is medium and SampEn-T8 is low and PermEn-T7 is high	41%	84.25%
If PhEn-FP2 is low and PeFP2 is high	40%	79.65%
If PhEn-FP2 is high and SampEn-T8 is medium and PermEn-T7 is low	30%	75.45%

Rule for fear	Coverage	Accuracy
If PhEn-T7 is Low, sampEn-T8 Medium, PHFP2 is Medium	55%	72.29%
If PhEn-T7 is medium, sampT8 Medium, PHFP2 is Medium	52%	70.42%

Rule for neutrality	Coverage	Accuracy
If PhEn-FP2 is medium and SampEn-T8 is medium and PermEn-T7 is high	55%	75.23%
If PhEn-FP2 is medium and SampEn-T8 is high and PermEn-T7 is medium	45%	70.45%
If PhEn-FP2 is low and SampEn-T8 is medium and PermEn-T7 is low	43%	74.25%

TABLE 8. Comparison of recent machine learning ER studies from same databases.

Ref	Database	Method	Evaluation method	Classes	Accuracy (%)
[60]	MAHNOB-HCI	PSD, RFE, GNB,	10-fold CV	Arousal, valence	66.7 (arousal), 80 (valence)
[61]	MAHNOB-HCI	Power spectrum, SVM	LOSO[1] CV	Arousal, valence	55.72 (valence), 60.23 (arousal)
[62]	MAHNOB-HCI	SP, KNN, SVM	LOSO CV	Arousal, valence	63 (valence), 65.1 (arousal)
[63]	SEED-IV	Granger causality-Transfer entropy, KNN	LOSO CV	sad, happy, fear, neutral	90
[24]	SEED-IV	Multi-branch EEG and eye feature fusion	5-fold CV	sad, happy, fear, neutral	87.32
[7]	SEED-IV	EEG: PSD, DE. Eye movements: pupil diameters, fixation details, saccade details, blink details, and event statistics, multimodal deep learning, FLF	Hold out CV	happy, sad, fear, and neutral	85.11
[27]	SEED-IV	EEG:1-D convolution kernels. Eye movements: pupil diameter, blink duration, Fixation duration, dispersion, SOFNN	5-fold CV	sad, happy, fear, neutral	86.27
Ours (2024)	SEED-IV, MAHNOB-HCI	Wavelet transform, entropies, mRMR, S-FIS-GA	5-fold CV	4 (sad, happy, fear, neutral)	94.42 (SEED-IV), 85.20 (MAHNOB-HCI)

memories are stored and recalled based on their emotional content.

Also, selected EEG channels base on mRMR method, T7, T8 and Fp2, are consistent with recent ER studies on SEED-IV database [7], [55], [57], [58], [59]. For example, Zheng et al., [7] present EmotionMeter, a multimodal emotion recognition framework combining brain waves and eye movements. For real-world feasibility and wearability, they designed a six-electrode included T7, T8 and four near ears electrodes to collect EEG signals. By integrating EEG and eye movements, they enhanced recognition accuracy by merging users' cognitive states and subconscious behaviors. Also, Zheng and Lu [55] found that these two channels are appropriate between a large number of healthy subjects to recognize sadness and happiness. They created time-frequency synchrosqueezing wavelet transform images and used pre-trained CNN models to recognize these emotional classes.

D. EMOTIONAL RULES

TABLE 7 reports selected rules for each class resultant five frequency bands of delta, theta, alpha, beta and gamma for both databases. According to this table, for sadness, there are three rules with varying levels of coverage and accuracy and the first rule, achieved the coverage of 57% and an accuracy of 75.78%. For fear, two rules are presented and the first rule achieved the coverage of 55% coverage and an accuracy of 72.29%. For happiness, several rules with decreasing levels of coverage from 58% to 30% are shown, and their accuracies range from 82.65% to 75.45%. For neutrality, three rules are listed and the first rule achieved the coverage of 55% and an accuracy of 75.23%.

E. COMPARISON WITH MULTIMODAL STUDIES

TABLE 8 present a comparison of recent machine learning studies on ER from the same databases, with a focus on their methodologies, evaluation methods, number of classes, and accuracy percentages. Our study utilizing both SEED-IV and MAHNOB-HCI databases, shows a substantial improvement over previous works. Our method includes extracting SampleEn, PheEn, SymbEn, PermuEn features as input of S-FIS, then tuning S-FIS rules using GA. The evaluation was done using the 5-fold CV approach on 4 emotional classes—sad, happy, fear, and neutral. The accuracy achieved was 94.42% for SEED-IV and 85.2% for MAHNOB-HCI, significantly higher than previous studies. For instance, Koelstra and Patras [50] using PSD and SVM and achieved the accuracy of 80% for valence and 66.7% for arousal on the MAHNOB-HCI database. Compared to the closest competitor in SEED-IV, Fu et al. [24] used multi-branch EEG and eye feature fusion with a 5-fold CV, our method demonstrates a notable improvement: from their 87.32% accuracy to our 94.42%. The significant jump in accuracy in our 2024 study highlights the effectiveness of our approach, combining multimodal information and advanced feature extraction techniques to understand and classify complex emotional states with high accuracy.

F. ADVANTAGE, DISADVANTAGE AND LIMITATIONS OF THE STUDY

The study has several advantages:

-It selects more effective EEG segments based on the eye-gate strategy, reducing computational demands and costs, enabling the use of less expensive processors in multi-modal wearable ER systems since full EEG processing is unnecessary.

Based on the findings of the manuscript, we suggest that an AI wearable ER system, such as hands-free glasses equipped with simple eye-tracking technology to measure and calculate a single feature (average pupil diameter in the Y direction), can comfortably and user-friendly recognize four desired emotions: sadness, happiness, fear, and neutral.

-The adaptability of the S-FIS-GA-ER system allows for tuning the rules knowledge base on new databases without starting from scratch.

-The study successfully integrates and understands fuzzy rules within the ER challenge, introducing uncertainty management into the problem.

The study's disadvantages include:

The S-FIS's limited input capacity. While machine learning methods typically generate and select features from a large pool for classification, FIS uses fewer inputs, which could lead to underutilization of S-FIS despite its usefulness in managing uncertainty in ER.

The study's limitations are:

The scarcity of multimodal databases combining eye-tracking and EEG signals is a primary limitation in ER research. Although valuable databases like MAHNOB-HCI [9] and the SEED series [7], [8] exist, they have limitations such as the SEED series being recorded in three separate sessions with only 15 subjects watching a considerable number of emotional clips (72 clips for SEED-IV). To improve validity, future studies should include more subjects from diverse cultures, ages, and genders.

VI. CONCLUSION

In this study, an interesting idea based on gated strategy by eye track data is proposed to identify specific timing of eliciting emotions. This timing has been investigated through common eye track features such as pupil diameter using the mRMR selection technique. Then, EEG signals are processed at this corresponding time and entropy features such as PhEn is extracted from five standard frequency bands which were decomposed using wavelet transform method. Next important step was mining fuzzy rules using a designed S-FIS and tuned by GA. Most discriminative rules caused the average accuracy of 94.42% and 85.2% at alpha frequency bands for the SEED-IV and MAHNOB-HCI databases, respectively.

The results in this article are presented in two ways: 1-the results related to the extracted knowledge base for each frequency band whose signal follows the eye gate strategy and the results related to the selected rules for each class. 2-It should be noted that the fuzzy design was adaptive so that after the construction of the basic knowledge base, the parameters of the system can be adjusted and there is no need for another design for new databases.

In the future, we will try to reduce EEG channels based on more effective channels to have a comfort wearable ER device from EEG signals and eye track data. Also, we will add extra modalities such as electrocardiogram (ECG) or electrodermal activity signals to improve performance of real-time ER systems. Moreover, lightweight deep learning approach such as autoencoders and long-short term memory (LSTM) techniques will be used to extract and decode deeper features from EEG signals.

STATEMENTS AND DECLARATIONS

COMPETING INTERESTS

The authors declare that they have no known competing financial interests or personal relationships that could have appeared to influence the work reported in this paper. Also, there are no financial supports or funds for this research.

REFERENCES

[1] B. García-Martínez, A. Martínez-Rodrigo, R. Alcaraz, and A. Fernández-Caballero, "A review on nonlinear methods using electroencephalographic recordings for emotion recognition," *IEEE Trans. Affect. Comput.*, vol. 12, no. 3, pp. 801–820, Jul. 2021.

[2] M. M. Rahman, A. K. Sarkar, M. A. Hossain, M. S. Hossain, M. R. Islam, M. B. Hossain, J. M. W. Quinn, and M. A. Moni, "Recognition of human emotions using EEG signals: A review," *Comput. Biol. Med.*, vol. 136, Sep. 2021, Art. no. 104696.

[3] M. Jafari, A. Shoeibi, M. Khodatars, S. Bagherzadeh, A. Shalbaf, D. L. García, J. M. Gorriz, and U. R. Acharya, "Emotion recognition in EEG signals using deep learning methods: A review," *Comput. Biol. Med.*, vol. 165, Oct. 2023, Art. no. 107450.

[4] A. Wabnegger, R. Ille, P. Schwingenschuh, P. Katschnig-Winter, M. Kögl-Wallner, K. Wenzel, and A. Schienle, "Facial emotion recognition in Parkinson's disease: An fMRI investigation," *PLoS ONE*, vol. 10, no. 8, Aug. 2015, Art. no. e0136110.

[5] M. K. Abadi, R. Subramanian, S. M. Kia, P. Avesani, I. Patras, and N. Sebe, "DECAF: MEG-based multimodal database for decoding affective physiological responses," *IEEE Trans. Affect. Comput.*, vol. 6, no. 3, pp. 209–222, Jul. 2015.

[6] Y. Hoshi, J. Huang, S. Kohri, Y. Iguchi, M. Naya, T. Okamoto, and S. Ono, "Recognition of human emotions from cerebral blood flow changes in the frontal region: A study with event-related near-infrared spectroscopy," *J. Neuroimag.*, vol. 21, no. 2, pp. e94–e101, Apr. 2011.

[7] W.-L. Zheng, W. Liu, Y. Lu, B.-L. Lu, and A. Cichocki, "EmotionMeter: A multimodal framework for recognizing human emotions," *IEEE Trans. Cybern.*, vol. 49, no. 3, pp. 1110–1122, Mar. 2019.

[8] W. Liu, J.-L. Qiu, W.-L. Zheng, and B.-L. Lu, "Comparing recognition performance and robustness of multimodal deep learning models for multimodal emotion recognition," *IEEE Trans. Cognit. Develop. Syst.*, vol. 14, no. 2, pp. 715–729, Jun. 2022.

[9] M. Soleymani, J. Lichtenauer, T. Pun, and M. Pantic, "A multimodal database for affect recognition and implicit tagging," *IEEE Trans. Affect. Comput.*, vol. 3, no. 1, pp. 42–55, Jan. 2012.

[10] I. Setien-Ramos, J. Lugo-Marín, L. Gisbert-Gustemps, E. Díez-Villoria, M. Magán-Maganto, R. Canal-Bedia, and J. A. Ramos-Quiroga, "Eye-tracking studies in adults with autism spectrum disorder: A systematic review and meta-analysis," *J. Autism Develop. Disorders*, vol. 53, no. 6, pp. 2430–2443, Jun. 2023.

[11] Q. Wei, H. Cao, Y. Shi, X. Xu, and T. Li, "Machine learning based on eye-tracking data to identify autism spectrum disorder: A systematic review and meta-analysis," *J. Biomed. Informat.*, vol. 137, Jan. 2023, Art. no. 104254.

[12] H. Chang, Y. Zong, W. Zheng, C. Tang, J. Zhu, and X. Li, "Depression assessment method: An EEG emotion recognition framework based on spatiotemporal neural network," *Frontiers Psychiatry*, vol. 12, Mar. 2022, Art. no. 837149.

[13] C.-T. Wu, D. G. Dillon, H.-C. Hsu, S. Huang, E. Barrick, and Y.-H. Liu, "Depression detection using relative EEG power induced by emotionally positive images and a conformal kernel support vector machine," *Appl. Sci.*, vol. 8, no. 8, p. 1244, Jul. 2018.

[14] G. Giannakakis, D. Grigoriadis, and M. Tsiknakis, "Detection of stress/anxiety state from EEG features during video watching," in *Proc. 37th Annu. Int. Conf. IEEE Eng. Med. Biol. Soc. (EMBC)*, Aug. 2015, pp. 6034–6037.

[15] Z. Li, X. Wu, X. Xu, H. Wang, Z. Guo, Z. Zhan, and L. Yao, "The recognition of multiple anxiety levels based on electroencephalograph," *IEEE Trans. Affect. Comput.*, vol. 13, no. 1, pp. 519–529, Jan. 2022.

[16] L. Bai, J. Guo, T. Xu, and M. Yang, "Emotional monitoring of learners based on EEG signal recognition," *Proc. Comput. Sci.*, vol. 174, pp. 364–368, Jan. 2020.

[17] Y. Ding, X. Chen, S. Zhong, and L. Liu, "Emotion analysis of college students using a fuzzy support vector machine," *Math. Problems Eng.*, vol. 2020, no. 1, 2020, Art. no. 8931486.

[18] G. Du, W. Zhou, C. Li, D. Li, and P. X. Liu, "An emotion recognition method for game evaluation based on electroencephalogram," *IEEE Trans. Affect. Comput.*, vol. 14, no. 1, pp. 591–602, Jan. 2023.

[19] W.-L. Zheng, B.-N. Dong, and B.-L. Lu, "Multimodal emotion recognition using EEG and eye tracking data," in *Proc. 36th Annu. Int. Conf. IEEE Eng. Med. Biol. Soc.*, Aug. 2014, pp. 5040–5043.

[20] Y. Su, W. Li, N. Bi, and Z. Lv, "Adolescents environmental emotion perception by integrating EEG and eye movements," *Frontiers Neurorobot.*, vol. 13, p. 46, Jun. 2019.

[21] T.-H. Li, W. Liu, W.-L. Zheng, and B.-L. Lu, "Classification of five emotions from EEG and eye movement signals: Discrimination ability and stability over time," in *Proc. 9th Int. IEEE/EMBS Conf. Neural Eng. (NER)*, Mar. 2019, pp. 607–610.

[22] X. Gong, C. L. P. Chen, and T. Zhang, "Cross-cultural emotion recognition with EEG and eye movement signals based on multiple stacked broad learning system," *IEEE Trans. Computat. Social Syst.*, vol. 11, no. 2, pp. 2014–2025, Aug. 2023.

[23] S. Zhu, J. Qi, J. Hu, and S. Hao, "A new approach for product evaluation based on integration of EEG and eye-tracking," *Adv. Eng. Informat.*, vol. 52, Apr. 2022, Art. no. 101601.

[24] B. Fu, C. Gu, M. Fu, Y. Xia, and Y. Liu, "A novel feature fusion network for multimodal emotion recognition from EEG and eye movement signals," *Frontiers Neurosci.*, vol. 17, Aug. 2023, Art. no. 1234162.

[25] Y. Lu, W. L. Zheng, B. Li, and B. L. Lu, "Combining eye movements and EEG to enhance emotion recognition," in *Proc. IJCAI*, vol. 15, 2015, pp. 1170–1176.

[26] E. Antoniou, P. Bozios, V. Christou, K. D. Tzimourta, K. Kalafatakis, M. G. Tsipouras, N. Giannakeas, and A. T. Tzallas, "EEG-based eye movement recognition using brain–computer interface and random forests," *Sensors*, vol. 21, no. 7, p. 2339, Mar. 2021.

[27] S. Zhou, D. Huang, C. Liu, and D. Jiang, "Objectivity meets subjectivity: A subjective and objective feature fused neural network for emotion recognition," *Appl. Soft Comput.*, vol. 122, Jun. 2022, Art. no. 108889.

[28] P. Ekman, "Basic emotions," in *Handbook Cognition Emotion*, vol. 98, 1999, pp. 45–60.

[29] A. Malekzadeh, A. Zare, M. Yaghoobi, and R. Alizadehsani, "Automatic diagnosis of epileptic seizures in EEG signals using fractal dimension features and convolutional autoencoder method," *Big Data Cognit. Comput.*, vol. 5, no. 4, p. 78, Dec. 2021.

[30] S. G. Mallat, "A theory for multiresolution signal decomposition: The wavelet representation," *IEEE Trans. Pattern Anal. Mach. Intell.*, vol. 11, no. 7, pp. 674–693, Jul. 1989.

[31] P. Patel and R. N. Annavarapu, "EEG-based human emotion recognition using entropy as a feature extraction measure," *Brain Informat.*, vol. 8, no. 1, p. 20, Dec. 2021.

[32] Y. You, W. Chen, M. Li, T. Zhang, Y. Jiang, and X. Zheng, "Automatic focal and non-focal EEG detection using entropy-based features from flexible analytic wavelet transform," *Biomed. Signal Process. Control*, vol. 57, Mar. 2020, Art. no. 101761.

[33] J. J. Żebrowski, W. Popławska, R. Baranowski, and T. Buchner, "Symbolic dynamics and complexity in a physiological time series," *Chaos, Solitons Fractals*, vol. 11, no. 7, pp. 1061–1075, Jun. 2000.

[34] A. Rohila and A. Sharma, "Phase entropy: A new complexity measure for heart rate variability," *Physiol. Meas.*, vol. 40, no. 10, Nov. 2019, Art. no. 105006.

[35] P. T. Krishnan, A. N. Joseph Raj, P. Balasubramanian, and Y. Chen, "Schizophrenia detection using MultivariateEmpirical mode decomposition and entropy measures from multichannel EEG signal," *Biocybern. Biomed. Eng.*, vol. 40, no. 3, pp. 1124–1139, Jul. 2020.

[36] X. Jie, R. Cao, and L. Li, "Emotion recognition based on the sample entropy of EEG," *Bio-Med. Mater. Eng.*, vol. 24, no. 1, pp. 1185–1192, 2014.

[37] F. Kaffashi, R. Foglyano, C. G. Wilson, and K. A. Loparo, "The effect of time delay on approximate & sample entropy calculations," *Phys. D, Nonlinear Phenomena*, vol. 237, no. 23, pp. 3069–3074, 2008.

[38] L. A. Zadeh, "Fuzzy logic," in *Granular, Fuzzy, and Soft Computing*. New York, NY, USA: Springer, 2023, pp. 19–49.

[39] H. J. Zimmermann, "Fuzzy set theory," *Wiley Interdiscipl. Rev., Comput. Statist.*, vol. 2, no. 3, pp. 317–332, 2010.

[40] J. Espinosa, J. Vandewalle, and V. Wertz, "Constructing fuzzy models from input-output data," in *Fuzzy Logic, Identification and Predictive Control* (Advances in Industrial Control). London, U.K.: Springer, 2005, pp. 21–58.

[41] M. Goudarzi and K. Maghooli, "Extraction of fuzzy rules at different concept levels related to image features of mammography for diagnosis of breast cancer," *Biocybern. Biomed. Eng.*, vol. 38, no. 4, pp. 1004–1014, 2018.

[42] M. Sugeno, *Industrial Applications of Fuzzy Control*. Amsterdam, The Netherlands: Elsevier, 1985.

[43] J. Saini, M. Dutta, and G. Marques, "Fuzzy inference system tree with particle swarm optimization and genetic algorithm: A novel approach for PM_{10} forecasting," *Expert Syst. Appl.*, vol. 183, Nov. 2021, Art. no. 115376.

[44] S. Mirjalili, "Genetic algorithm," in *Evolutionary Algorithms and Neural Networks: Theory and Applications*. Cham, Switzerland: Springer, 2019, pp. 43–55.

[45] T. Mitsuishi, "Definition of centroid method as defuzzification," *Formalized Math.*, vol. 30, pp. 125–134, 2022.

[46] M. Sokolova and G. Lapalme, "A systematic analysis of performance measures for classification tasks," *Inf. Process. Manage.*, vol. 45, no. 4, pp. 427–437, Jul. 2009.

[47] M. Oliva and A. Anikin, "Pupil dilation reflects the time course of emotion recognition in human vocalizations," *Sci. Rep.*, vol. 8, no. 1, p. 4871, Mar. 2018.

[48] R. Takano and M. Nomura, "A closer look at the time course of bodily responses to awe experiences," *Sci. Rep.*, vol. 13, no. 1, p. 22506, Dec. 2023.

[49] A. T. Duchowski, *Eye Tracking Methodology: Theory and Practice*, 3rd ed. London, U.K.: Springer-Verlag. 2017.

[50] J. Polich, "Updating P300: An integrative theory of P3a and P3b," *Clin. Neurophysiol.*, vol. 118, no. 10, pp. 2128–2148, 2007.

[51] A. Wolf, K. Ueda, and Y. Hirano, "Recent updates of eye movement abnormalities in patients with schizophrenia: A scoping review," *Psychiatry Clin. Neurosci.*, vol. 75, no. 3, pp. 82–100, Mar. 2021.

[52] A. W. Joseph and R. Murugesh, "Potential eye tracking metrics and indicators to measure cognitive load in human-computer interaction research," *J. Sci. Res.*, vol. 64, no. 1, pp. 168–175, 2020.

[53] S. Bagherzadeh, K. Maghooli, A. Shalbaf, and A. Maghsoudi, "Recognition of emotional states using frequency effective connectivity maps through transfer learning approach from electroencephalogram signals," *Biomed. Signal Process. Control*, vol. 75, May 2022, Art. no. 103544.

[54] D. Leite, V. Frigeri Jr., and R. Medeiros, "Incremental fuzzy machine learning for online classification of emotions in games from EEG data streams," in *Handbook on Computer Learning and Intelligence: Deep Learning, Intelligent Control and Evolutionary Computation*, 2022, pp. 235–262.

[55] W.-L. Zheng and B.-L. Lu, "Investigating critical frequency bands and channels for EEG-based emotion recognition with deep neural networks," *IEEE Trans. Auto. Mental Develop.*, vol. 7, no. 3, pp. 162–175, Sep. 2015.

[56] F. Demir, N. Sobahi, S. Siuly, and A. Sengur, "Exploring deep learning features for automatic classification of human emotion using EEG rhythms," *IEEE Sensors J.*, vol. 21, no. 13, pp. 14923–14930, Jul. 2021.

[57] S. Bagherzadeh, M. R. Norouzi, S. Bahri Hampa, A. Ghasri, P. Tolou Kouroshi, S. Hosseininasab, M. A. Ghasem Zadeh, and A. M. Nasrabadi, "A subject-independent portable emotion recognition system using synchrosqueezing wavelet transform maps of EEG signals and ResNet-18," *Biomed. Signal Process. Control*, vol. 90, Apr. 2024, Art. no. 105875.

[58] A. Dogan, P. D. Barua, M. Baygin, T. Tuncer, S. Dogan, O. Yaman, A. H. Dogru, and R. U. Acharya, "Automated accurate emotion classification using clefia pattern-based features with EEG signals," *Int. J. Healthcare Manage.*, vol. 17, no. 1, pp. 32–45, Jan. 2024.

[59] T. Tuncer, S. Dogan, and A. Subasi, "LEDPatNet19: Automated emotion recognition model based on nonlinear LED pattern feature extraction function using EEG signals," *Cognit. Neurodynamics*, vol. 16, no. 4, pp. 779–790, Aug. 2022.

[60] S. Koelstra and I. Patras, "Fusion of facial expressions and EEG for implicit affective tagging," *Image Vis. Comput.*, vol. 31, no. 2, pp. 164–174, Feb. 2013.

[61] Y. Zhu, S. Wang, and Q. Ji, "Emotion recognition from users' EEG signals with the help of stimulus VIDEOS," in *Proc. IEEE Int. Conf. Multimedia Expo (ICME)*, Jul. 2014, pp. 1–6.

[62] X. Huang, J. Kortelainen, G. Zhao, X. Li, A. Moilanen, T. Seppänen, and M. Pietikäinen, "Multi-modal emotion analysis from facial expressions and electroencephalogram," *Comput. Vis. Image Understand.*, vol. 147, pp. 114–124, Jun. 2016.

[63] J. S. Ramakrishna, N. Sinha, and H. Ramasangu, "Classification of human emotions using EEG-based causal connectivity patterns," in *Proc. IEEE Conf. Comput. Intell. Bioinf. Comput. Biol. (CIBCB)*, Oct. 2021, pp. 1–8.

JAVID FARHADI SEDEHI received the B.Sc. degree in biomedical engineering from Islamic Azad University, Dezful, in 2014, and the M.Sc. degree in biomedical engineering from the Science and Research Branch, Islamic Azad University, Tehran, Iran, in 2016, where he is currently pursuing the Ph.D. degree. His research interests include biomedical signal processing, imaging technique, fuzzy systems, machine learning, and deep learning techniques.

NADER JAFARNIA DABANLOO received the B.Sc. degree in electrical engineering from Tehran University, in 1988, the M.Sc. degree in electrical engineering from Khajeh Nasir Toosi University of Technology, in 1996, and the Ph.D. degree in biomedical engineering from Iran University of Science and Technology, in 2005. Currently, he is a Professor of biomedical engineering with the Science and Research Branch, Islamic Azad University, Tehran, Iran. His research interests include biomedical signal processing, modeling biological systems, advanced neural networks, and cognitive neuroscience.

KEIVAN MAGHOOLI received the B.Sc. degree in electrical engineering from Iran University of Science and Technology, in 1995, the M.Sc. degree in electrical engineering from Tarbiat Modares University, in 1999, and the Ph.D. degree in biomedical engineering from the Science and Research Branch, Islamic Azad University, Tehran, Iran, in 2003. Currently, he is an Associate Professor of biomedical engineering with the Science and Research Branch, Islamic Azad University. His research interests include biomedical signal processing, fuzzy systems, data mining, pattern recognition, and cognitive neuroscience.

ALI SHEIKHANI received the B.Sc. degree in electrical engineering major communication from the Amirkabir University of Technology, in 1992, the M.Sc. degree in electrical engineering major communication from Islamic Azad University, Tehran, Iran, in 1996, and the Ph.D. degree in biomedical engineering from the Science and Research Branch, Islamic Azad University, in 2000. Currently, he is an Assistance Professor of biomedical engineering with the Science and Research Branch, Islamic Azad University. His research interests include biomedical signal processing especially electroencephalogram, digital signal processing, machine learning, and cognitive neuroscience.